# Simultaneous measurement of intracellular $Ca^{2+}$ and asynchronous transmitter release from the same crayfish bouton

R. Ravin, M. E. Spira, H. Parnas and I. Parnas*

*The Otto Loewi Centre for Cellular and Molecular Neurobiology, Department of Neurobiology, The Hebrew University, Jerusalem 91904, Israel*

1. A technique has been developed to monitor neurotransmitter release simultaneously with intracellular $Ca^{2+}$ concentration ($[Ca^{2+}]_i$) in single release boutons whose diameters range from 3 to 5 $\mu$m.

2. Using this technique, we have found a highly non-linear relationship between the rate of asynchronous release and $[Ca^{2+}]_i$. The Hill coefficient lies between 3 and 4.

3. The affinity ($K_d$) of the putative release-related $Ca^{2+}$ receptor for asynchronous release was calculated to be in the range of 2–4 $\mu$M.

4. The same range of values of Hill coefficient and $K_d$ were obtained when $[Ca^{2+}]_i$ was elevated both by bath application of ionomycin and by repetitive stimulation at high frequency.

5. Our results show that the $Ca^{2+}$ receptor(s) associated with asynchronous release exhibits high affinity for $Ca^{2+}$.

The pioneering work of Katz and his colleagues (Katz, 1969) established that $Ca^{2+}$ plays a key role in release of neurotransmitter but the exact nature of this role is still under debate (for reviews see Augustine, Charlton & Smith, 1987; Parnas, Parnas & Segel, 1990; Linial & Parnas, 1996). It is essential to know the affinity of the putative $Ca^{2+}$ receptor(s) for calcium in order to understand the role calcium plays in the process of neurotransmitter release and to identify unambiguously the molecules or molecular complexes to which it binds. Unfortunately, the available imaging techniques have insufficient spatial and temporal resolution to detect rapid changes in free intracellular calcium concentration ($[Ca^{2+}]_i$) near the $Ca^{2+}$ channels and the release sites. Several mathematical models have therefore been advanced to calculate the $Ca^{2+}$ concentration below and in the vicinity of a $Ca^{2+}$ channel. According to these models, $[Ca^{2+}]_i$ may reach values of hundreds of micromolar at the inner face of the calcium channels and a concentration as high as 100 $\mu$M near the release sites (Fogelson & Zucker, 1985; Simon & Llinas, 1985; Yamada & Zucker, 1992). From such calculations the authors mentioned above concluded that the $Ca^{2+}$ receptor molecule must have a low affinity for $Ca^{2+}$, lying in the range of tens to hundreds of micromolar. This conclusion was recently supported by Llinas, Sugimori & Silver (1995) who reported that, in the squid giant synapse, evoked release is associated with an increase in $[Ca^{2+}]_i$ to 300–400 $\mu$M for periods of 800 $\mu$s in restricted submembrane domains.

However, in contrast, other mathematical models that, like the models above, take tail currents and endogenous buffers into account (Aharon, Parnas & Parnas, 1994; Aharon, Bercovier & Parnas, 1996) have shown that high $Ca^{2+}$ concentrations are virtually confined to the area of the channel mouth. $Ca^{2+}$ concentration drops tenfold just a few nanometers away. The $Ca^{2+}$ concentration was calculated to be even lower 50 nm away from the inner face of the calcium channel where the release sites are assumed to be situated (Fogelson & Zucker, 1985). Accordingly, these models predict that the release mechanism has a high affinity for calcium.

This issue can only be resolved by experimentally determining the $K_d$ of the putative $Ca^{2+}$ receptor(s). This can be done by establishing the quantitative relationship between $[Ca^{2+}]_i$ and neurotransmitter release in a single release bouton. Such data are difficult to obtain for evoked release, because transient local concentrations of calcium cannot be monitored with available techniques, as mentioned above.

Measurement of asynchronous release avoids these difficulties. Asynchronous release, like evoked release, depends on the concentration of $Ca^{2+}$ near the release sites. The theoretical work of Aharon *et al.* (1994) shows that, in a nerve terminal of 1 $\mu$m diameter, $Ca^{2+}$ entering through a $Ca^{2+}$ channel is distributed rather homogeneously (in a shell of tens of nanometres around the channel) even microseconds after the end of the pulse (Fig. 11 of Aharon *et al.* 1994). Using the

* To whom correspondence should be addressed.

same method of calculation for the crayfish release bouton (see Methods) it is safe to conclude that, for asynchronous release, which follows the period of evoked release, the cytosolic $Ca^{2+}$ concentration is rather homogeneous 3 ms after the pulse and reflects the $Ca^{2+}$ concentration near the release sites. Keeping in mind that the $Ca^{2+}$ receptor might not be the same for evoked and asynchronous release (Geppert *et al.* 1994), we investigate here the simpler case of the relationship between $[Ca^{2+}]_i$ and asynchronous release. The experimental system required for such measurements must enable simultaneous monitoring of $[Ca^{2+}]_i$ and asynchronous neurotransmitter release from the same release bouton. This can be done in only very few preparations. For example, the release boutons of the excitatory axon innervating the crayfish opener muscle are suitable for such a study. These crayfish release boutons, or varicosities, are relatively small (3–5 $\mu$m; Fig. 2), and they can be filled with $Ca^{2+}$ indicators to monitor $[Ca^{2+}]_i$. In an earlier study, Delaney, Zucker & Tank (1989), measured their intracellular $Ca^{2+}$ concentration while monitoring evoked release with an intracellular electrode in the postsynaptic muscle cell. However, the excitatory axon in crustaceans forms many release boutons on each muscle fibre (Fatt & Katz, 1953) and therefore an intracellular electrode in the muscle cell detects release from many boutons. Because different boutons on the same muscle fibre have different release properties (Cooper, Marin & Atwood, 1995; Parnas, Dudel, Parnas & Ravin, 1996) recording asynchronous release with an intracellular electrode may not be adequate for extrapolating the $K_d$ of the $Ca^{2+}$ receptor molecule, even though it is technically easier. In the study presented here, we were able to measure asynchronous release simultaneously with $[Ca^{2+}]_i$ from the same bouton. We found that as $[Ca^{2+}]_i$ rises the rate of asynchronous release increases sigmoidally with a Hill coefficient ranging between 3 and 4. This value is similar to that found for the dependence of evoked release on extracellular $Ca^{2+}$ concentration in the frog (Dodge & Rahamimoff, 1967) and in crayfish (Parnas, Parnas & Dudel, 1982), on intracellular $Ca^{2+}$ concentration (Zucker Delaney, Mulkey & Tank, 1991; Lando & Zucker, 1994), or on $Ca^{2+}$ currents (Smith, Augustine & Charlton, 1985) in the squid. We could also extract a value of 2–4 $\mu$M for the $K_d$ of the putative asynchronous release-related $Ca^{2+}$ receptor from our measurements. These results show that the calcium receptor(s) associated with asynchronous release exhibits high affinity for $Ca^{2+}$.

## METHODS

### Preparation

Experiments were performed on the opener muscle of the first walking leg (which was removed by autotomy) of the crayfish *Procambarus clarki*. Animals 3–4 cm long were purchased from Atchafalaya Biological Supply (Raceland, LA, USA). The preparation, with its exposed excitor axon and opener muscle (Wojtowitcz & Atwood, 1984), was glued (Delaney *et al.* 1989) to a microscope slide that served as the bottom of a perfusion chamber (total volume, 0·4 ml). The chamber was placed on a microscope stage (Optiphot 2, Nikon, Tokyo) and the preparation was constantly superfused by means of a peristaltic pump (Gilson minipulse 3, France). Perfusion was with a van Harreveld solution composed of (mM): NaCl, 220; KCl, 5·4; $CaCl_2$, 13·5; $MgCl_2$, 2·5; Tris, 10; pH adjusted to 7·4 with NaOH. After the injection of fura-2, 500 nM TTX was added to prevent sodium action potentials. The bath temperature was kept at 11 ± 0·5 °C.

### Experimental procedure

Four micromanipulators were attached to the stage of the microscope. One was used to hold a glass rod with a fine tip to support a secondary branch of the excitatory axon, the second was used for the fura-2 intra-axonal injecting microelectrode, a third hydraulic micromanipulator (MHW-3, Narishige, Tokyo) held the macropatch electrode, and the fourth held a suction electrode to stimulate the isolated nerve bundle containing the excitatory axon.

### Fura-2 and mag-fura-2 loading and visualization of single release boutons

Either a high affinity or a low affinity calcium indicator was used to monitor a wide range of $[Ca^{2+}]_i$ within single release boutons. We used fura-2 ($K_d$ = 850 nM, see below) for imaging low $[Ca^{2+}]_i$ in the range of 0·1–4 $\mu$M and mag-fura-2 ($K_d$ = 100 $\mu$M, see below) for imaging $[Ca^{2+}]_i > 25$ $\mu$M.

For fura injection, one of the secondary branches of the excitatory axon was impaled by a 20 MΩ microelectrode containing 200 mM KCl and 22 mM fura-2 pentapotassium or mag-fura-2 tetrapotassium (Molecular Probes). The indicator, was injected by passing 6–15 nA negative DC for 10–20 min. The final intra-axonal fura-2 concentration used in our experiments was 50–100 $\mu$M, and that of mag-fura-2, 50–130 $\mu$M. The intra-axonal concentration was estimated by comparing the indicator's fluorescence intensity in the axon branch with that of a glass capillary (same diameter as the branch) containing a solution with a known concentration of indicator. The solution was composed of (mM): KCl, 250; NaCl, 15; EGTA, 7; $CaCl_2$, 3·3; and Hepes, 15; pH 7·4. The ionic strength of this solution approximates the intracellular ionic strength of crayfish neurons (Wallin, 1967). Its final free $Ca^{2+}$ concentration was 100 nM. To estimate the intracellular fura-2 concentration we used an excitation wavelength of 360 nm and an emission filter of 510 nm. An excitation wavelength of 380 nm was used for mag-fura-2 calibration. The filled axon terminals with their varicosities became visible at the fura-2 or mag-fura-2 concentrations as above (Fig. 4*A*, for fura-2), enabling us to place the macropatch electrode over one of the varicosities under visual control (Fig. 4*A*). The seal resistance formed under these conditions was 200–250 kΩ.

### Calcium imaging

We followed the general procedure of Grynkiewicz, Poenie & Tsien, (1985) as described in detail by Ziv & Spira (1993, 1995). The fluorescence microscope system consisted of a 150 W xenon arc lamp (model 66002, Oriel, Stratford, CT, USA), an upright microscope (Optiphot 2) equipped with a long working distance ×40 objective (0·75 NA, Zeiss, Oberkochen, Germany), band-pass excitation filters of 360 ± 5 and 380 ± 5 nm, and a frame grabber (Imaging Technologies, Bedford, MA, USA). A computer-controlled Uniblitz electronic shutter was placed in the light path to reduce unnecessary exposure of a varicosity to the excitation light. Fluorescence images of a fura-2-loaded varicosity were obtained by brief exposure of the bouton to two excitation wavelengths of 360 and 380 nm. Mag-fura-2 was imaged with one wavelength as described previously by Neher & Augustine (1992).

The experimental protocol used to obtain fura-2 ratio images was as follows. A single varicosity was depolarized for 0·6–1 ms (for fura-2) or 5 ms (for mag-fura-2) by rectangular negative current pulses (Dudel, 1981) at a given frequency while transmitter release was monitored with the same electrode. Fluorescence images of the stimulated varicosity as well as nearby non-stimulated varicosities were monitored by an intensified CCD video camera (model 2400-77, Hamamatsu, Hamamatsu City, Japan) and stored on a $\frac{3}{4}$-inch videotape recorder (VTR) at a video rate of 1 frame per 33 ms (model Vo 9850P, Sony, Japan). The images were obtained before and throughout the stimulation period. At the end of the stimulation period, the excitation filter was switched to 360 nm (isosbestic point of fura-2) and fluorescence images were recorded by the VTR for 5–7 s. Background images of regions near the bouton were also recorded at both excitation wavelengths.

It is important to ensure that, at the time of sampling, the cytosolic $[Ca^{2+}]$ measured with our method indeed reflects the $Ca^{2+}$ concentration below the membrane. Using the same method of simulation as in Aharon *et al.* (1994), which allows consideration of the three-dimensional configuration and uses the finite elements method, we found that the spatial gradients of $Ca^{2+}$ had completely dissipated by 3 ms after the end of a 1 ms depolarizing pulse. These calculations were done for a release bouton (5 $\mu$m diameter) where $Ca^{2+}$ enters only through the membrane of half the bouton's surface. Other parameters such as the $Ca^{2+}$ diffusion coefficient, rate constants of buffers and initial $Ca^{2+}$ concentration were taken from Tank, Regehr & Delaney (1995), with the fixed buffer concentration being 1200 $\mu$M. The intracellular fura-2 concentration was taken as 100 $\mu$M. These calculations show that the $[Ca^{2+}]_i$ reflects the $Ca^{2+}$ concentration associated with asynchronous release.

### Fura-2 pseudocolour images production

Pseudocolour images of $[Ca^{2+}]_i$ were produced off-line as follows. The continuous VTR recording of the experiment was transformed into a series of images, each created by averaging thirty-two consecutive frames. A section of frame containing background fluorescence, but no boutons, was subtracted from the averaged images. The background-subtracted 360 nm images obtained after cessation of the stimulation were divided (pixel by pixel) by the series of background-subtracted 380 nm averaged images obtained before, during and after cessation of stimulation. The ratio images obtained in this way were then converted to pseudocolour images by an appropriate look-up table (Fig. 4*A*).

### Fura-2 $[Ca^{2+}]_i$ imaging at high temporal resolution

The following procedure was used to display the change in $[Ca^{2+}]_i$ at a higher temporal resolution (60 ms per point) in the form of graphs (Figs 4 and 5). While exciting at 380 nm, VTR frames before, during and after stimulation were grabbed, digitized and processed. For each frame, we fitted the largest possible square in the bouton (Fig. 4*A*) and this square remained constant (size and position) throughout the analysis of the bouton. Another constant square (size and position) near the bouton was used for subtracting the background. The procedure was then repeated, taking frames at 360 nm excitation after cessation of stimulation, and using the same subtraction procedure for the same squares. Thirty such subtraction images, taken at 360 nm, were averaged to obtain the final 360 nm value. This value was divided by the consecutive 380 nm values and the resulting ratio values were translated to calcium concentration as described by Grynkiewicz *et al.* (1985).

### Calcium imaging by mag-fura-2

High calcium concentrations were imaged by mag-fura-2 using the single excitation wavelength ratio procedure of Neher & Augustine (1992). The $K_d$ for their equation was evaluated from the calibration curve obtained as described below. This method is valid provided that the fluorescence signal is undisturbed by changes in the dimensions of the structure under study. In a series of experiments, we tested whether high frequency stimulation of a bouton induces changes in the bouton's volume. Imaging of boutons filled with sulphorhodamine-B (Molecular Probes Europe, Leiden, The Netherlands) while stimulating the boutons with 5 ms current pulses at 100 Hz did not induce noticeable changes in the fluorescence signals. Thus, we can conclude that high frequency stimulation does not induce changes in the bouton's morphology. (Grabbing, storing, and processing the mag-fura-2 images were performed as described above for fura-2.)

### Calibration of the fura-2 and mag-fura-2 signals

Two calibration curves were constructed (Fig. 1): a calibration curve (denoted *in vitro*) in buffer solutions designed to mimic crayfish axoplasm (Wallin, 1967) and a calibration curve within the axoplasm (denoted *in vivo*). A series of buffered solutions containing defined free $Ca^{2+}$ concentrations was prepared for the *in vitro* calibration, using the method of Bers (1982). The actual values of the free $Ca^{2+}$ concentration in the calibration solutions were verified by direct measurements with a $Ca^{2+}$-sensitive electrode (Orion 93-20, Orion, Boston, MA, USA). For the construction of a $Ca^{2+}$ calibration curve, 1·5 $\mu$l of each of the calibration solutions containing 22 $\mu$M fura-2 pentapotassium (or mag-fura-2 tetrapotassium, see below) were placed on a cover slide, imaged, and the ratio values for each solution were calculated. The values of the fluorescence ratio in the absence of $Ca^{2+}$ ($R_{min}$) and the fluorescence ratio at saturating $Ca^{2+}$ ($R_{max}$; Grynkiewicz *et al.* 1985) were obtained by using the $Ca^{2+}$-free buffer and a buffer containing 100 mM $CaCl_2$, respectively. A typical calibration curve for fura-2 is illustrated in Fig. 1*A*. The theoretical curve for fura-2 was produced according to eqn (5) of Grynkiewicz *et al.* (1985) in which the following measured values were used for fura-2: $R_{min} = 0{\cdot}46$, $R_{max} = 5{\cdot}3$, $Sf_2/Sb_2 = 18$, where $Sf_2$ is the fluorescence of the free indicator and $Sb_2$ is the fluorescence of the $Ca^{2+}$-bound indicator, both at 380 nm (for further details see Grynkiewicz *et al.* 1985). The best fit of the theoretical curve to the experimental points was obtained when the $K_d$ was set to 850 nM, a value close to that of 865 nM obtained by Delaney *et al.* (1991).

Since there has been concern about the effects of the axoplasm on the calibration parameters (see for example Ziv & Spira, 1995), we attempted to produce a fura-2 calibration curve within the axoplasm of the axon. To establish $R_{min}$, we bathed the axon in calcium-free van Harreveld solution containing 2 mM EGTA, for 1 h. The *in vivo* $R_{min}$ value obtained from the fura-2-loaded axon under these conditions was 0·46. To establish the *in vivo* $R_{max}$, an axon was equilibrated for 1 h in van Harreveld solution containing 50 mM carbonyl cyanide *m*-chlorophenyl hydrazone (CCCP; Sigma), 10 $\mu$M ionomycin and 13·5 $\mu$M $Ca^{2+}$. $R_{max}$ of about 5 was obtained under these conditions. The dashed curve of Fig. 1*A* was obtained using a $K_d$ of 850 nM. It should be noted that the two calibration curves are almost identical in the range of 50 nM to about 15 $\mu$M. We therefore used the *in vitro* calibration curves.

For the calibration of the mag-fura-2 signals we have used essentially the same procedure as for fura-2 with some modification. The isosbestic point for mag-fura-2 is 350 nm. Because of that the changes in the emission intensity of 360 and 380 nm excitation wavelengths are of the same sign. We have therefore used the ratio of readings obtained with excitation at 340 and 380 nm that produce changes in emission of an opposite sign (Fig. 1*B*).

The following values were measured for use with mag-fura-2: $R_{min} = 0{\cdot}07$, $R_{max} = 3{\cdot}74$, $Sf_2/Sb_2 = 36{\cdot}65$ and $K_d$ was set to 100 $\mu$M. The calculated curve closely fitted the experimental data (Fig. 1*B*). It should be noted that the mag-fura-2 calibration curve was obtained in the presence of 2·5 mM $Mg^{2+}$. Once the $K_d$ was obtained we introduced its value in the single excitation wavelength equation of Neher & Augustine (1992).

### Recording single quantum events

Single quantum events were recorded with the macropatch technique (Dudel, 1981). Because of the short distance (1·8 mm) between the objective lens and the preparation, macropatch electrodes with long shafts were pulled on a three-stage, computerized puller (DMZ, Universal Puller, Zietz-Instrument, Munich, Germany). The tips were slightly bent to allow the patch electrode a horizontal approach and were heat polished to form an opening of 8–10 $\mu$m diameter. The same macropatch electrode was used for recording and to depolarize the region below the electrode by passing extracellular negative constant current pulses of −0·5 to −1·2 $\mu$A for 0·5–5 ms (Dudel, 1981). The macropatch electrode sampled release from only the bouton below the electrode. We reached this conclusion because when the electrode was placed near a bouton it did not record any quanta events. Samples of recordings in Fig. 4*C* show a failure in release and one, three and four quanta. Traces were digitized at 50 kHz (Neuro-Corder, Neuro Data, NY, USA) and stored on video cassettes. Analysis was carried out with a Pentium computer (90 MHz) using the LabVIEW interface (National Instruments, Austin, TX, USA) and our own software for counting the number of quanta and measuring the delay to each quantum.

### Calculating the rate of asynchronous release

According to convention, we define asynchronous release as the release which occurs prior to a stimulating pulse and following termination of evoked release (Fig. 2). This means that the time course of evoked release must be established in order to distinguish evoked from asynchronous release. This was done by plotting synaptic delay histograms (Parnas *et al.* 1990) and Fig. 2 shows the synaptic delay histograms obtained at different frequencies of stimulation. Release at each frequency, given as the number of quanta obtained at different time bins before and after the stimulus, was measured during the period at which $[Ca^{2+}]_i$ reached its maximal steady-state level. As shown in Fig. 2, evoked release lasted 5 ms at all frequencies; that is, 5 ms after each pulse the rate of release decayed to about the same rate as before the pulse (see values in legends). Consequently, asynchronous release could be safely measured starting 5 ms after each stimulus. This also held for a stimulation frequency of 100 Hz.

### Chemicals

Fura-2 and mag-fura-2 were purchased from Molecular Probes. TTX was purchased from Sigma and RBI. Ionomycin was purchased from Calbiochem and Sigma.

## RESULTS

### $Ca^{2+}$ imaging through the macropatch electrode

We first determined whether placing a macropatch electrode over a varicosity distorts the ratio imaging of $[Ca^{2+}]_i$. After the injection of fura-2 into the axon to reach a final concentration of 50–100 $\mu$M, the $[Ca^{2+}]_i$ in the boutons was increased by adding 2 $\mu$M ionomycin to the bathing solution. The $[Ca^{2+}]_i$ increased gradually and sampling was taken at different times following ionomycin application. In twenty-five boutons, comparing $[Ca^{2+}]_i$ measured with the electrode over the bouton with the $[Ca^{2+}]_i$ measured without the electrode revealed no significant differences (Fig. 3). Thus,

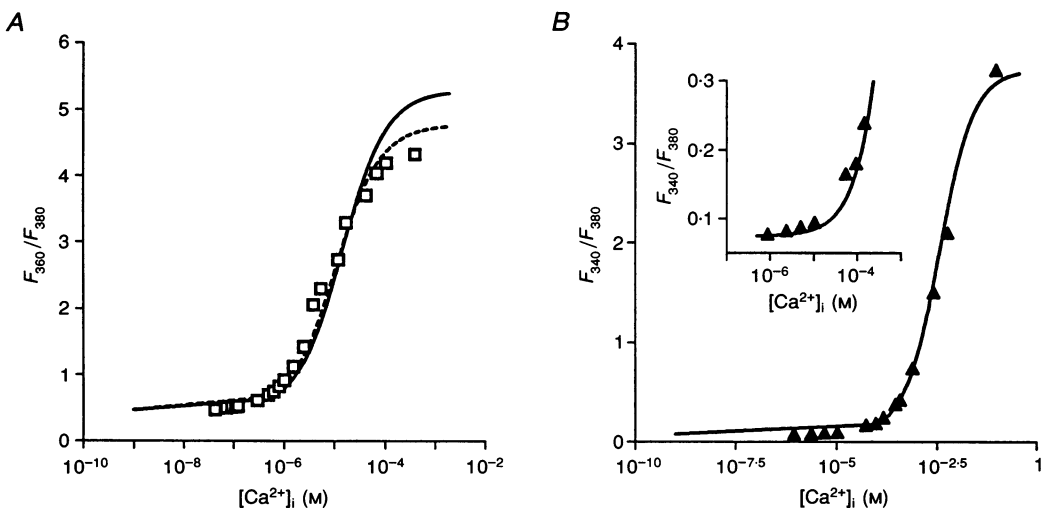


**Figure 1. Calibration curves for fura-2 and mag-fura-2**

*A*, calibration curve for fura-2. □, experimental data from *in vitro* experiments. Continuous line, theoretical, calculated curve using the constants obtained with the *in vitro* calibration. The fluorescence ratio in the absence of $Ca^{2+}$, $R_{min} = 0{\cdot}46$; the fluorescence ratio at saturating $Ca^{2+}$, $R_{max} = 5{\cdot}3$; $Sf_2 = 166{\cdot}2$; and $Sb_2 = 9{\cdot}3$. Dashed line, the theoretical calculated curve using the constants obtained from the *in vivo* calibration. $R_{min} = 0{\cdot}46$, $R_{max} = 4{\cdot}77$, $Sf_2 = 161{\cdot}6$ and $Sb_2 = 12{\cdot}8$. In both cases $K_d = 850$ nM. *B*, calibration curve for the mag-fura-2. ▲, experimental points from *in vitro* experiments. Continuous line, the theoretical curve using the constants obtained from the *in vitro* calibration. $R_{min} = 0{\cdot}07$, $R_{max} = 3{\cdot}73$, $Sf_2 = 178{\cdot}1$ and $Sb_2 = 4{\cdot}86$. $K_d = 100$ $\mu$M. Inset, expansion of the lower part of the curve.

placing the electrode over a release bouton does not distort the $[Ca^{2+}]_i$ measurement.

### Elevation of $[Ca^{2+}]_i$ by high frequency stimulation

Figure 4 shows the overall experimental procedure. After the injection of fura-2 (or mag-fura-2) into the axon, a macropatch electrode was placed over a single bouton under visual control (Fig. 4*A*). Trains of negative current pulses were delivered through the electrode at different frequencies (100 Hz in Fig. 4). The $[Ca^{2+}]_i$ (Fig. 4*B*) and quantal events (Fig. 4*C*) were monitored simultaneously. Figure 5 shows the rate of increase and maximal $[Ca^{2+}]_i$ in a bouton depolarized by pulses of 1 ms, −0·9 μA at five frequencies (20, 40, 60, 80 and 100 Hz). Plateau level and the rate of rise in $Ca^{2+}$ concentration were determined at each frequency. The beginning and end of the plateau were determined by eye, and the plateau level was given by the average of the fluctuating line (Fig. 5 inset). The rate of rise was measured for the straight line starting at a point 10% above the average baseline to 10% below the plateau level (Fig. 5 inset, dashed line). Because the number of pulses at the different frequencies was kept constant (700 pulses), the duration of stimulation became shorter as the frequency of stimulation increased. In this experiment, the rates of increase in $[Ca^{2+}]_i$ corresponding to the various frequencies were 0·16, 0·57, 1·01, 1·77 and 2·63 μM $s^{-1}$ for 20, 40, 60, 80 and 100 Hz, respectively. The plateau $[Ca^{2+}]_i$ values for the same frequencies were 0·97, 1·67, 2·37, 2·74 and 3·34 μM, respectively.

To check that at the high frequencies $[Ca^{2+}]_i$ did not reach the fura-2 saturation level, we increased $[Ca^{2+}]_i$ by applying ionomycin and the mitochondrial uncoupler CCCP to the bath. In the presence of ionomycin (1 μM) and CCCP

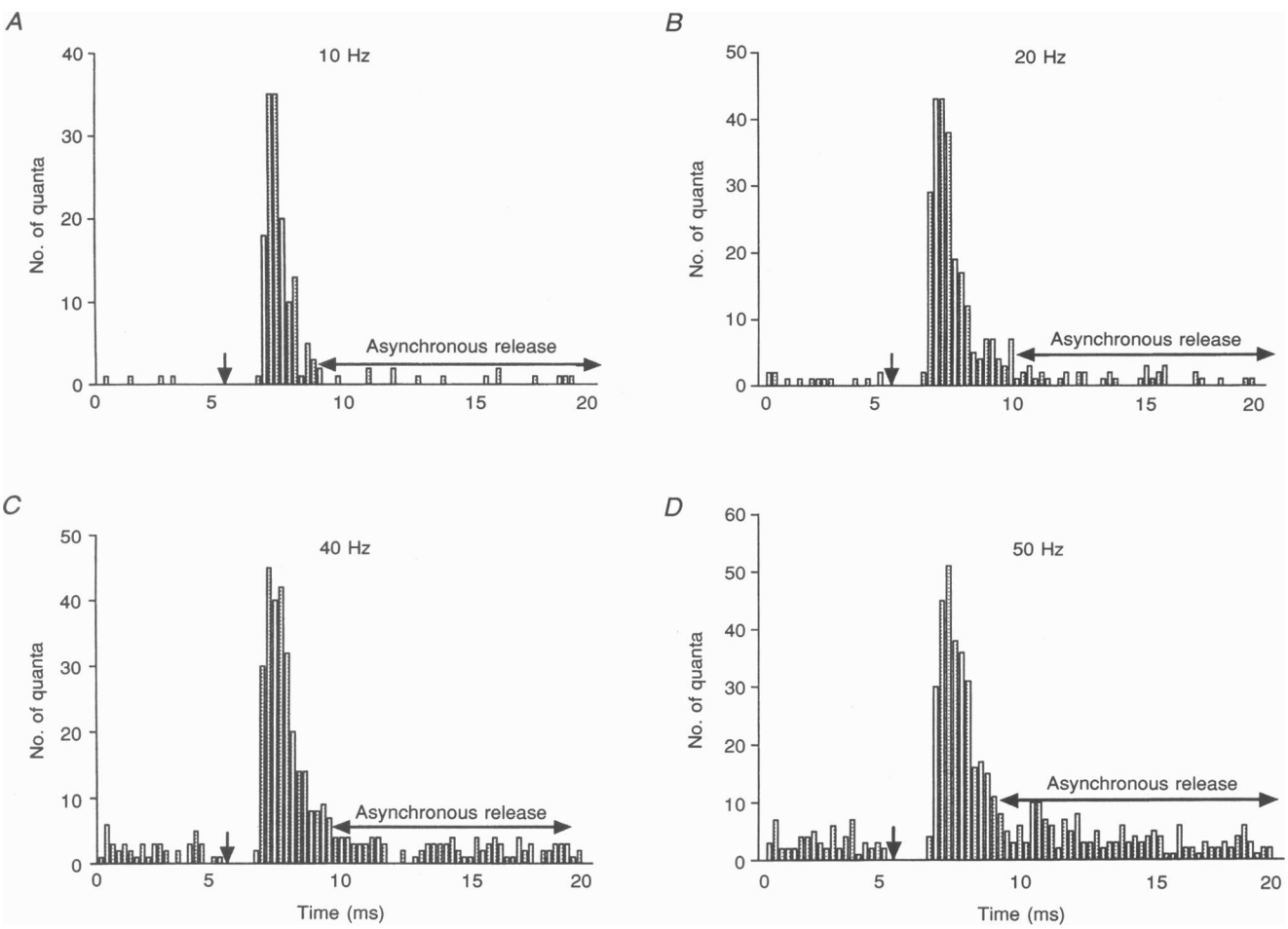


**Figure 2. Evoked and asynchronous release obtained at different stimulation frequencies**

The level of asynchronous release can be determined from synaptic delay histograms, obtained as follows. A single bouton was stimulated with a train of 1000 pulses (1 ms duration, −0·9 μA amplitude) at 10, 20, 40 and 50 Hz. The stimuli were applied at the time indicated by the vertical arrows. After each stimulus, the delay to each quantum was measured. The gap in the period between the arrow and the histogram is caused by the stimulus artifact; quanta cannot be detected during this time. These delay histograms show that evoked release lasted 5 ms at most, as the rate of asynchronous release, $S$ ($s^{-1}$), was similar before and 5 ms after each stimulus. These rates were, before and after, respectively: for 10 Hz, 1·24 and 1·38; 20 Hz, 2·88 and 3·35; 40 Hz, 8·61 and 8·74 and 50 Hz, 13·95 and 14·96. Note that the rate of asynchronous release increased with frequency of stimulation.

(20 $\mu$M), $[Ca^{2+}]_i$ increased to levels higher than 10 $\mu$M and this elevation was detected by fura-2 (not shown). For higher levels of $[Ca^{2+}]_i$ we used mag-fura-2 (see Fig. 7).

### Dependence of the rate of asynchronous release on $[Ca^{2+}]_i$

$[Ca^{2+}]_i$ in the bouton was raised either by trains of depolarizing pulses (Figs 4 and 5) or by application of ionomycin. Figure 6 shows results where $S$, the rate of asynchronous release, was measured at various $[Ca^{2+}]_i$. In Fig. 6*A*, $[Ca^{2+}]_i$ was raised by electrical stimulation. $S$ clearly increased in a non-linear fashion as $[Ca^{2+}]_i$ rose. The Hill coefficient, the slope of $\log S/\log[Ca^{2+}]_i$, was found to be $2{\cdot}77 \pm 0{\cdot}27$ (Fig. 6*B*). The average slope for twenty-two such experiments was $3{\cdot}29 \pm 0{\cdot}84$ ($n = 22$). Figure 6*C* shows results from another bouton (in another preparation) where $[Ca^{2+}]_i$ was raised by application of 2 $\mu$M ionomycin. Again $S$ increased in a sigmoidal manner as $[Ca^{2+}]_i$ rose. However, $S$ decreased once $[Ca^{2+}]_i$ reached levels of a few micromolar, even though $[Ca^{2+}]_i$ continued to increase. In Fig. 6*C*, $S$ reached about 120 $s^{-1}$ at a $[Ca^{2+}]_i$ of approximately 5 $\mu$M and then declined as $[Ca^{2+}]_i$ continued to increase. Plotting $\log S/\log[Ca^{2+}]_i$ for the ascending part of the graph in Fig. 6*C* gave a Hill coefficient of $3{\cdot}07 \pm 0{\cdot}16$ (Fig. 6*D*). In eight such experiments, the average slope was $3{\cdot}13 \pm 0{\cdot}89$ ($n = 8$). Note that a similar slope was obtained whether $[Ca^{2+}]_i$ was raised by ionomycin or by electrical stimulation. The value of the Hill coefficient is similar to that obtained for evoked release using extracellular $Ca^{2+}$ concentration, $[Ca^{2+}]_o$, in the frog (Dodge & Rahamimoff, 1967) and in the crayfish neuromuscular junction (Parnas *et al.* 1982), and for $[Ca^{2+}]_i$ in the crayfish (Lando & Zucker, 1994).

### Evaluation of $K_s$

The dependence of $S$ on $[Ca^{2+}]_i$ can be empirically described by:

$$S = \frac{\bar{S}[Ca^{2+}]_i^{n_s}}{(K_s + [Ca^{2+}]_i)^{n_s}}. \quad (1)$$

Here, $S$ denotes the rate of asynchronous release, $\bar{S}$ the maximal possible rate of asynchronous release at high $[Ca^{2+}]_i$, $n_s$ the Hill coefficient and $K_s$ the analogue of the half-saturation constant where the Hill coefficient equals 1. Equation (1) has a similar form to that describing the dependence of evoked release on extracellular $Ca^{2+}$

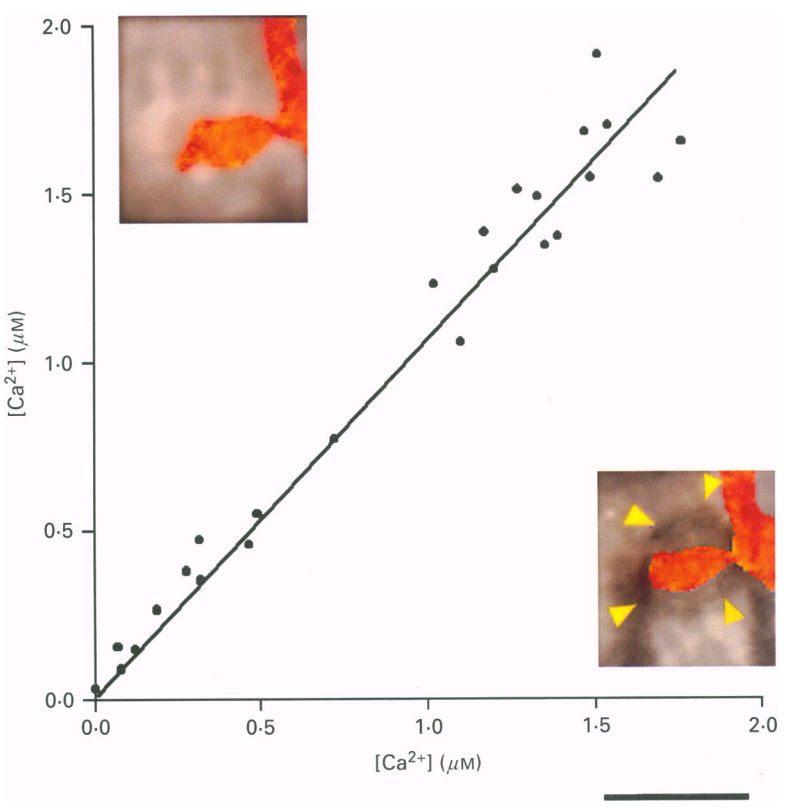


**Figure 3. The macropatch electrode does not distort $[Ca^{2+}]_i$ ratio imaging**

For these measurements the $[Ca^{2+}]_i$ was increased from 100 nM to about 1·6 $\mu$M by addition of 2 $\mu$M ionomycin to the bathing solution. For twenty-five boutons, the $[Ca^{2+}]_i$ was measured without the electrode as a control ($y$-axis), and then the macropatch electrode was placed over the bouton ($x$-axis). The electrode was then removed and an additional control (no electrode) value established. The slope of the linear regression line relating the 'control' and 'electrode' readings is 1·06, $r^2 = 0{\cdot}98$. The two insets show the bouton in the control situation without the electrode (upper left) and with the electrode over it (lower right). Yellow arrowheads point to the electrode rim. Calibration bar, 12 $\mu$m.

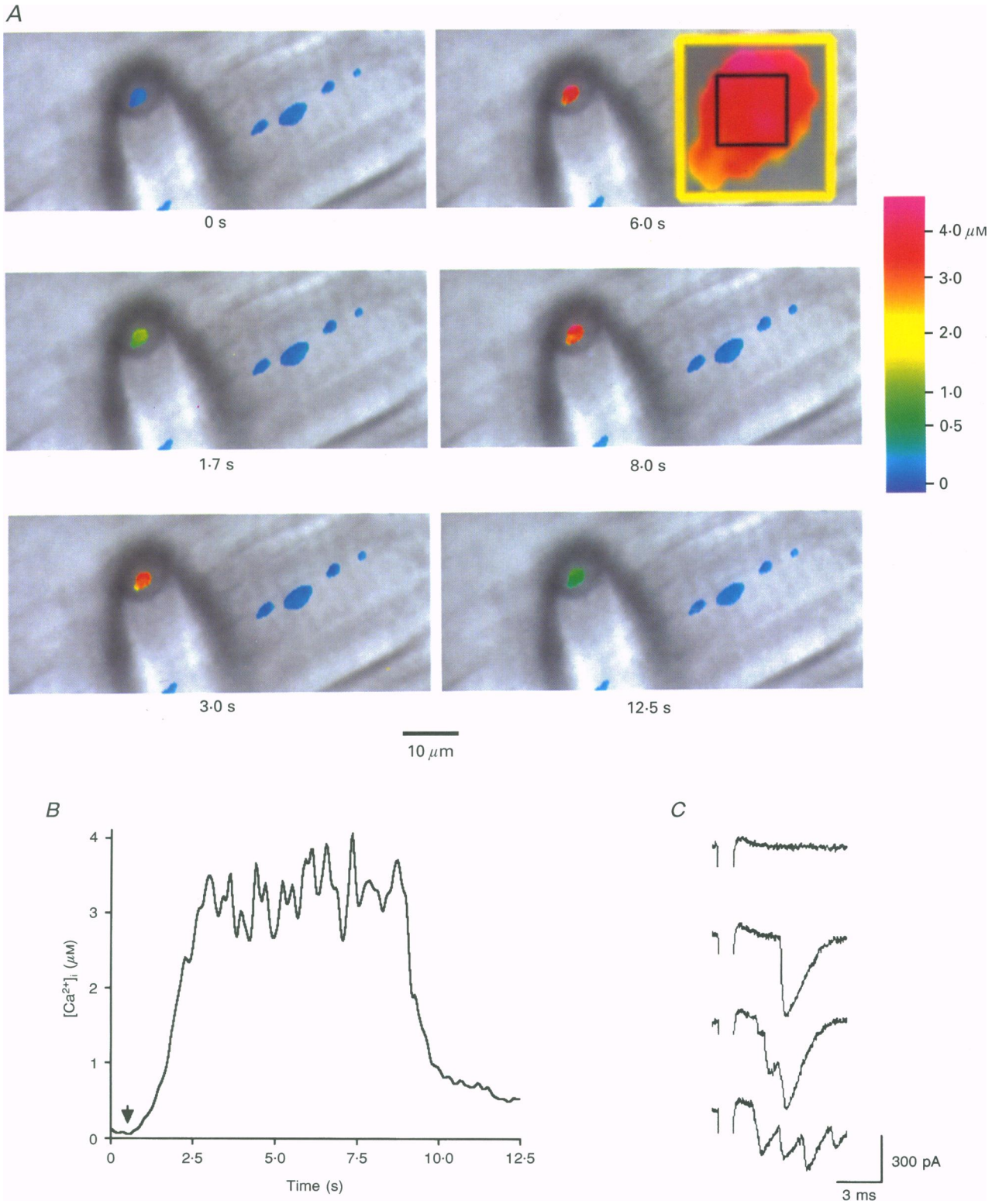


**Figure 4. Simultaneous recordings of $[Ca^{2+}]_i$ and excitatory postsynaptic currents (EPSCs) from a single bouton**

*A*, the fura-2 ratio image of the boutons was digitally superimposed upon a bright field image of the same field; see the macropatch electrode placed over a single bouton. Images were taken before, during and after a train of depolarizing pulses of 0·6 ms duration and −0·7 μA amplitude given for 8 s, at 100 Hz. The time at which the samples were taken is indicated in each frame. The square in the upper right frame depicts the area from which $[Ca^{2+}]_i$ was averaged. *B*, changes in $[Ca^{2+}]_i$ during the train of pulses and during recovery. The arrow represents beginning of stimulation. *C*, samples of quantal events recorded while $[Ca^{2+}]_i$ remained at the plateau level (2·5–8 s).

concentration (Dodge & Rahamimoff, 1967) and on intracellular $Ca^{2+}$ concentration (Parnas & Segel, 1980).

In principle, $K_s$ could be measured directly provided that a continuous curve describing the relationship between $S$ and a wide range of $[Ca^{2+}]_i$ could be determined for each bouton. This goal is impossible to achieve if only one calcium indicator is used. We therefore conducted separate experiments for the different ranges of $[Ca^{2+}]_i$. Fura-2 was used at low concentrations (a few micromolar), while mag-fura-2 was used for concentrations higher than 20 $\mu$M. We did not measure $[Ca^{2+}]_i$ at the intermediate $Ca^{2+}$ concentrations because fura-2 exhibits saturation and mag-fura-2 is still rather insensitive in this range.

Figure 7 shows results of such measurements. The values of $S$ for the low $[Ca^{2+}]_i$ are given in Fig. 7*A*. Figure 7*B* shows the full scale experiment with $S$ values obtained at high $[Ca^{2+}]_i$ in addition to the $S$ values of Fig. 7*A*. The continuous curves in Fig. 7*A* and *B* were obtained by fitting eqn (1) to the experimental points. To do so, two out of the three unknowns in eqn (1) had to be determined. An $S$ value of 500 $s^{-1}$ was derived from the experimental results (Fig. 7*B*). The Hill coefficient $n_s$ was also derived from the experimental results (Fig. 6 and average results); as it was larger than 3, we used a value of 4. With these two parameters fixed, the only remaining free parameter is $K_s$. The value of $K_s$ that best fitted the experimental data was 2·3 $\mu$M. To explore further the range of $K_s$ that still fits the experimental data, we tried $K_s = 1$ $\mu$M (dashed line in Fig. 7*A* and *B*) and 5 $\mu$M (dotted–dashed line in Fig. 7*A* and *B*). Taking into account the possible deviations in the experimental results we can safely conclude that the $K_s$ is in the range of 1–5 $\mu$M. In considering the meaning of $K_s$, it should be noted that only when $n_s = 1$, $K_s$ is the half-saturation constant for release. When $n_s > 1$, then $K_s$ corresponds to the $[Ca^{2+}]_i$ where $S = \bar{S}/2^{n_s}$.

$K_s$ can also be extracted from the data in Fig. 7*A* and *B* in a different way. Rearrangement of eqn (1) gives:

$$\frac{1}{S^{1/n_s}} = \left(\frac{K_s}{\bar{S}^{1/n_s}}\right)\left(\frac{1}{[Ca^{2+}]_i}\right) + \left(\frac{1}{\bar{S}^{1/n_s}}\right). \quad (2)$$

Equation (2) shows that plotting $1/S^{1/n_s}$ as a function of $1/[Ca^{2+}]_i$ will generate a straight line with a slope of $K_s/\bar{S}^{1/n_s}$ and its intersection with the $y$-axis provides $1/\bar{S}^{1/n_s}$.

This method allows indirect derivation of $\bar{S}$ and does not require reaching relatively high $[Ca^{2+}]_i$.

Figure 7*C* shows results from two such experiments, each from a different bouton. In one, $[Ca^{2+}]_i$ was raised by electrical stimulation, and in the other, by application of 2 $\mu$M ionomycin. The values for both experiments are plotted according to eqn (2). $\bar{S}$ was obtained from the point of intersection of the regression line with the $y$-axis. Taking $n_s = 4$, $\bar{S}$ was found to be 544 $s^{-1}$ for the experiment with electrical stimulation and 625 $s^{-1}$ for the ionomycin experiment. Using these values in eqn (2) we found $K_s$ to be 2·6 $\mu$M for the experiment with the electrical stimulation and 2·3 $\mu$M for the ionomycin experiment. Pooling all data with electrical stimulation ($n = 22$) and ionomycin ($n = 8$) (Fig. 7*D*), and from the regression line and its intersection point with the $y$-axis, we established the average $\bar{S}$ as 677 $s^{-1}$. The average $K_s$ was found to be 3·09 $\mu$M. The $\bar{S}$ value obtained with this method is quite similar to that measured directly from the maximal rate of release (Fig. 7*B*).

In conclusion it is obvious that $K_s$ values between 2 and 4 $\mu$M best fit the cumulative experimental data. This result stands whether $K_s$ is extracted using the rearranged eqn (2) or is derived by fitting eqn (1) to the bulk of the raw, non-linear experimental data (with electrical stimulation and ionomycin).

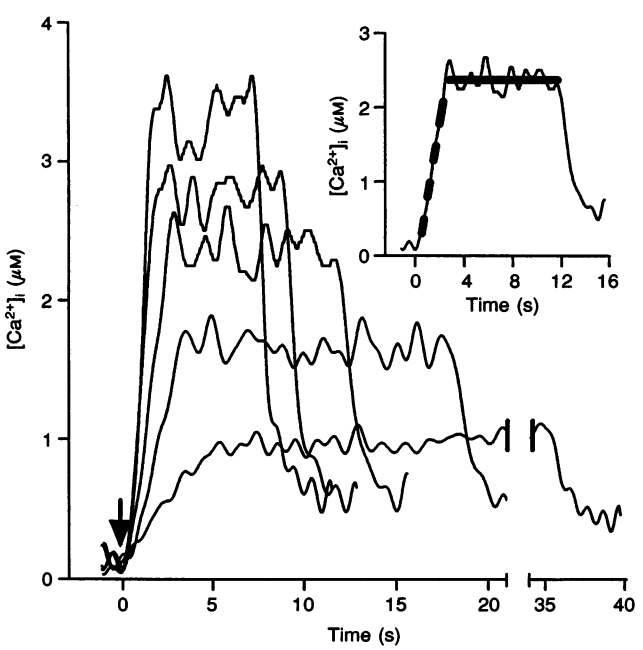


**Figure 5. $[Ca^{2+}]_i$ at different stimulation frequencies**
Increase in $[Ca^{2+}]_i$ in a single bouton stimulated with a train of 700 pulses (0·6 ms, −0·7 $\mu$A) at five frequencies (20, 40, 60, 80 and 100 Hz). The arrow marks the onset of the train of pulses. Inset shows how rise time (thick dashed line, −10 to 90% peak) and maximal level of $[Ca^{2+}]_i$ (continuous line) were measured.

## DISCUSSION

The $[Ca^{2+}]_i$ and the rate of asynchronous neurotransmitter release within a single bouton were measured simultaneously. We found a direct non-linear correlation between $[Ca^{2+}]_i$ and the rate of asynchronous release. This finding reinforces earlier studies arguing that the bulk cytoplasmic $Ca^{2+}$ concentration reflects the submembrane $Ca^{2+}$ concentration which controls the rate of asynchronous release (Miledi, 1973; Rahamimoff, Meiri, Erulkar & Barenholz, 1978).

For electrical stimulation our method to establish the cytosolic $Ca^{2+}$ concentration suffers from an inherent inaccuracy. Dye imaging was conducted using fairly long sampling intervals that include periods of both evoked and asynchronous release. Thus, the $[Ca^{2+}]_i$ obtained from dye emission may overestimate the $[Ca^{2+}]_i$ present during asynchronous release. The good agreement between the electrical stimulation and ionomycin data suggests that the overestimate is not severe.

In our experiments, asynchronous release was detected only when the steady-state $[Ca^{2+}]_i$ reached levels of 600–700 nM. The maximal rate of asynchronous release lay between 500 and 700 $s^{-1}$. This value is much lower than the value of 11 000 $s^{-1}$ obtained by Mulkey & Zucker (1993), a difference presumably explained by different recording techniques. Mulkey & Zucker (1993) recorded release from many nerve terminals innervating the same muscle fibre; we, in contrast, measured release from a single bouton. In the crayfish the excitatory terminal forms twenty to fifty synapses over a single muscle fibre (Fischer & Parnas, 1996) and so a rate of about 500–700 quanta $s^{-1}$ for a single bouton may indicate that Mulkey & Zucker (1993) recorded

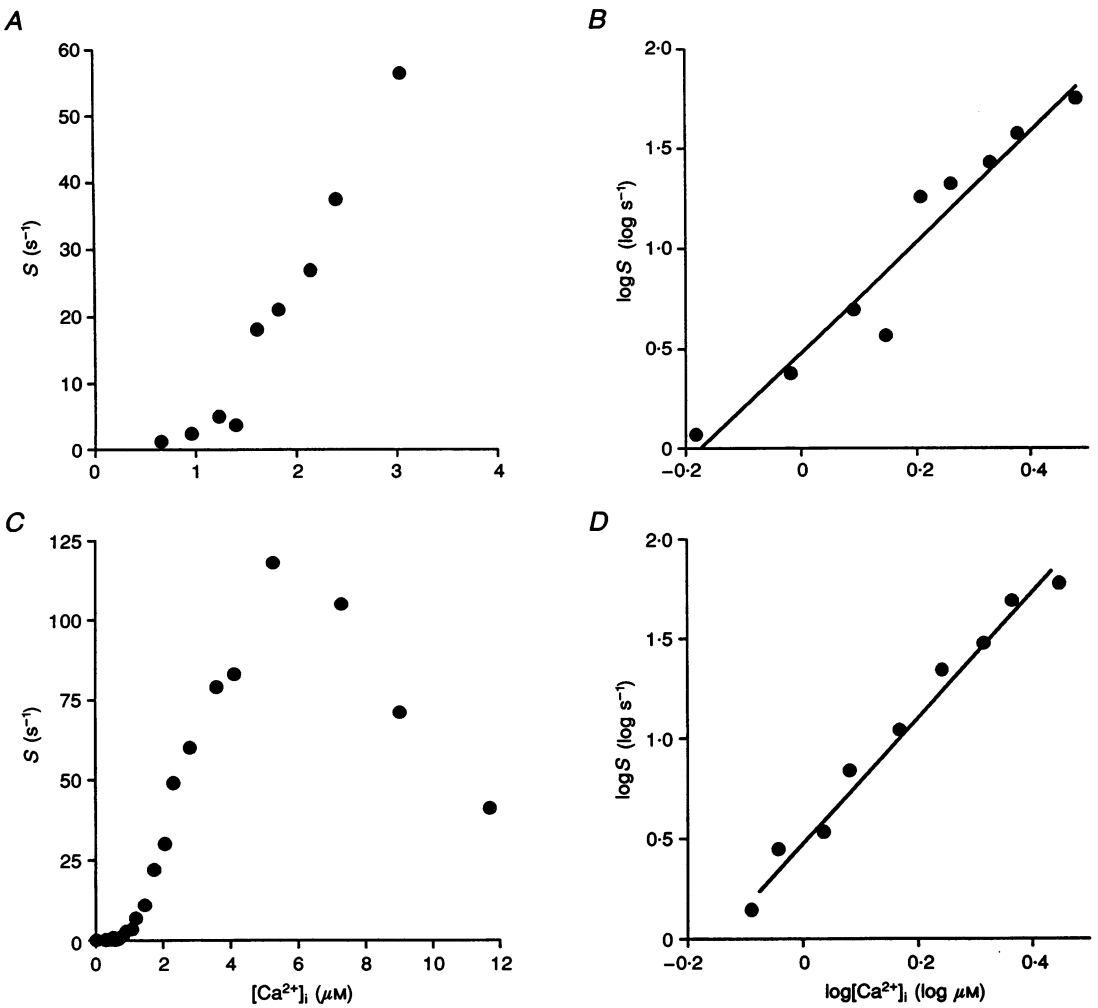


**Figure 6. Rate of asynchronous release, *S*, as a function of $[Ca^{2+}]_i$**

*A*, $[Ca^{2+}]_i$ was increased by stimulating one bouton (1 ms, −0·9 μA, 1000 pulses) at 9 frequencies (20, 30, 40, 50, 60, 70, 80, 90 and 100 Hz). $[Ca^{2+}]_i$ on the *x*-axis corresponds to maximal $[Ca^{2+}]_i$ at the various frequencies (see Fig. 5). Asynchronous release was measured during the corresponding period when $[Ca^{2+}]_i$ reached its maximal level. *B*, log–log plot of the results shown in *A* (slope = 2·77 ± 0·27 S.D.). *C*, rate of asynchronous release when $[Ca^{2+}]_i$ was increased in a bouton, from a different preparation, by application of 2 μM ionomycin to the external solution. *D*, log–log plot of the rising phase in *C* (slope = 3·07 ± 0·16 S.D.).

release from up to twenty of these twenty to fifty boutons (assuming equal release properties of boutons).

Our results indicate that the putative $Ca^{2+}$ binding protein for asynchronous release in the crayfish has a high affinity for $Ca^{2+}$. Irrespective of the two methods used the $K_d$ ($K_s$ in our notation) is in the range of a few micromolar. These results should be compared with earlier reports where $[Ca^{2+}]_i$ was raised homogeneously in the axon terminal or in the whole cell, e.g. by whole cell perfusion or flash photolysis. Mulkey & Zucker (1993) calculated that the $[Ca^{2+}]_i$ increased to the micromolar level in axon terminals of the crayfish neuromuscular junction injected with DM nitrophen and subjected to photolysis. Both evoked and asynchronous release increased markedly at this $Ca^{2+}$ concentration; the rate of asynchronous release increasing from 1–10 quanta $s^{-1}$ to 420–12 500 quanta $s^{-1}$ after photolysis and without nerve stimulation. These results suggest that, in the crayfish, the $Ca^{2+}$ receptor(s) associated with asynchronous release exhibits high affinity for $Ca^{2+}$.

However, in simulations of the $Ca^{2+}$ profiles obtained after photolysis of synaptic boutons loaded with DM nitrophen (opener neuromuscular junction of crayfish), Lando & Zucker (1994) found that the $Ca^{2+}$ concentration reached a peak of about 70 $\mu$M and then decayed to a level of about

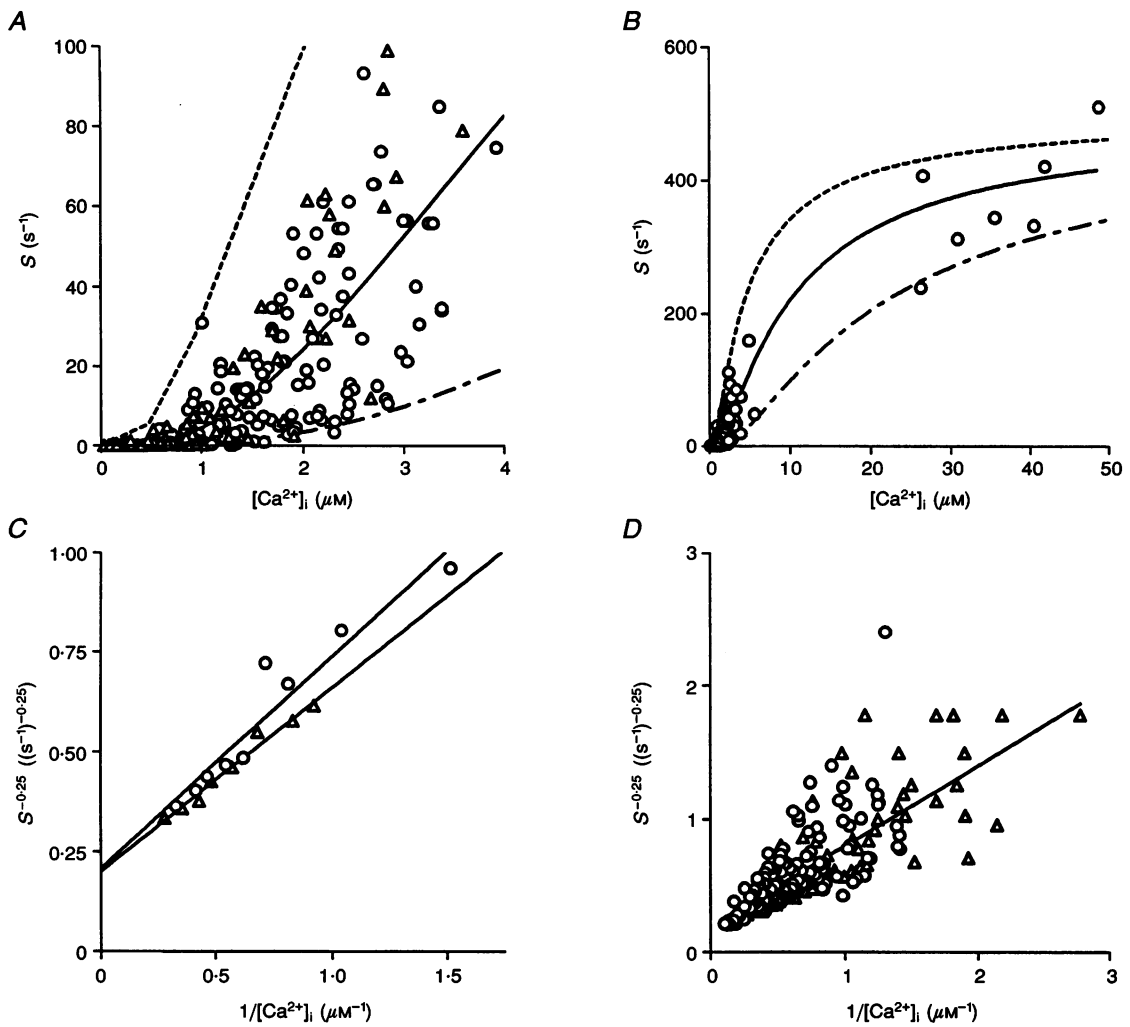


**Figure 7. Evaluation of $K_s$ and $\bar{S}$**

*A*, *S* as a function of $[Ca^{2+}]_i$ where $[Ca^{2+}]_i$ was measured with fura-2 (pooled results). △, $[Ca^{2+}]_i$ increased by ionomycin; ○, electrical stimulation. *B*, fura-2 and mag-fura-2 measurements. The data in the lower range of the curve are those of *A*, where for the higher levels of $[Ca^{2+}]_i$ mag-fura-2 was employed (pooled results). In *A* and *B* the regression lines were obtained using eqn (1). The continuous line depicts the best fit with the experimental data ($r^2 = 0{\cdot}89$); $K_s = 2{\cdot}3$ $\mu$M. For the dashed line, $K_s = 1$ $\mu$M; for the dotted–dashed line, $K_s = 5$ $\mu$M. For all lines $\bar{S} = 500\ s^{-1}$ and $n_s = 4$. It is clear that $K_s$ of 2·3 mM (continuous line) best fits the experimental data. *C*, results obtained from two boutons each from a different preparation. Symbols as above. Linear regression lines are based on eqn (2). The values of the parameters obtained are for ionomycin, $K_s = 2{\cdot}3$ $\mu$M and $\bar{S} = 625\ s^{-1}$; for electrical stimulation, $K_s = 2{\cdot}6$ $\mu$M and $\bar{S} = 544\ s^{-1}$. *D*, same data as in *A*, as given by eqn (2). Linear regression line is based on eqn (2). $\bar{S} = 677\ s^{-1}$ and $K_s = 3{\cdot}1$ $\mu$M.

10–12 $\mu$M in approximately 3 ms (Fig. 5 of Lando & Zucker, 1994). As they did not measure asynchronous release we cannot compare these later results with those of Mulkey & Zucker (1993) or with our present results.

There are also differences in the results obtained from 'slow' releasing systems such as chromaffin cells. Augustine & Neher (1992) found a significant rate of release when $[Ca^{2+}]_i$ reached levels of a few micromolar. Yet, Heinemann, Chow, Neher & Zucker (1994) also using chromaffin cells, calculated the $K_d$ of the $Ca^{2+}$ receptor to lie in the range of 7–21 $\mu$M and found that the half-saturation $Ca^{2+}$ concentration for release was about 40 $\mu$M.

It is not clear whether these differences arise mainly from genuine differences in the biological systems or are due to the indirect nature of the measurements. This can be resolved only by direct measurement. The experiments presented here are, to our knowledge, the first where release and intracellular $Ca^{2+}$ concentration have been measured directly and simultaneously from a single release bouton of a fast synapse. Our results show that the putative $Ca^{2+}$ receptor in crayfish boutons responsible for asynchronous release has a high affinity for $Ca^{2+}$ and that the $K_d$ lies in the range of a few micromolar.


Aharon, S., Bercovier, M. & Parnas, H. (1996). Parallel computation enables precise description of $Ca^{2+}$ distribution in nerve terminals. *Bulletin of Mathematical Biology* **58**, 1075–1097.

Aharon, S., Parnas, H. & Parnas, I. (1994). The magnitude and significance of $Ca^{2+}$ domains for release of neurotransmitter. *Bulletin of Mathematical Biology* **56**, 1095–1119.

Augustine, G. J., Charlton, M. P. & Smith, S. J. (1987). Calcium action in synaptic transmitter release. *Annual Review of Neuroscience* **10**, 633–693.

Augustine, G. J. & Neher, E. (1992). Calcium requirements for secretion in bovine chromaffin cells. *Journal of Physiology* **450**, 247–271.

Bers, D. M. (1982). A simple method for the accurate determination of free [Ca] in Ca-EGTA solutions. *American Journal of Physiology* **242**, C404–408.

Cooper, R. L., Marin, L. & Atwood, H. L. (1995). Synaptic differentiation of a single motor neuron: conjoint definition of transmitter release. Presynaptic calcium signals and ultrastructure. *Journal of Neuroscience* **15**, 4209–4222.

Delaney, K. R., Zucker, R. S. & Tank, D. W. (1989). Calcium in motor nerve terminals associated with posttetanic potentiation. *Journal of Neuroscience* **9**, 3558–3567.

Delaney, K. R., Tank, D. W. & Zucker, R. S. (1991). Presynaptic calcium and serotonin-mediated enhancement of transmitter release at crayfish neuromuscular junction. *Journal of Neuroscience* **11**, 2631–2643.

Dodge, F. A. & Rahamimoff, R. (1967). Cooperative action of calcium ions in transmitter release at the neuromuscular junction. *Journal of Physiology* **193**, 419–432.

Dudel, J. (1981). The effect of reduced calcium on quantal unit current and release at the crayfish neuromuscular junction. *Pflügers Archiv* **391**, 35–40.

Fatt, P. & Katz, B. (1953). Distributed end plate potentials of crustacean muscle fibers. *Journal of Experimental Biology* **30**, 433–439.

Fischer, Y. & Parnas, I. (1996). Differential activation of two distinct mechanisms for presynaptic inhibition by a single inhibitory axon. *Journal of Neurophysiology* **76**, 3807–3816.

Fogelson, A. L. & Zucker, R. S. (1985). Presynaptic calcium diffusion from various arrays of single channels: implications for transmitter release and synaptic facilitation. *Biophysical Journal* **48**, 1003–1017.

Geppert, M., Goda, Y., Hammer, R. E., Li, C., Rosahl, T. H., Stevens, C. F. & Sudhof, T. C. (1994). Synaptotagmin I: A major $Ca^{2+}$ sensor for transmitter release at the central synapse. *Cell* **79**, 717–727.

Grynkiewicz, G., Poenie, M. & Tsien, R. Y. (1985). A new generation of $Ca^{2+}$ indicators with greatly improved fluorescence properties. *Journal of Biological Chemistry* **280**, 3440–3450.

Heinemann, C., Chow, R. H., Neher, E. & Zucker, R. S. (1994). Kinetics of the secretory response in bovine chromaffin cells following flash photolysis of caged $Ca^{2+}$. *Biophysical Journal* **67**, 2546–2557.

Katz, B. (1969). *The Release of Neuronal Transmitter Substance.* Charles C. Thomas, Springfield, IL, USA.

Lando, L. & Zucker, R. S. (1994). $Ca^{2+}$ cooperativity in neurosecretion measured using photolabile $Ca^{2+}$ chelators. *Journal of Neurophysiology* **72**, 825–830.

Linial, M. & Parnas, D. (1996). Deciphering neuronal secretion: tools of the trade. *Biochimica et Biophysica Acta* **1286**, 117–152.

Llinas, R., Steinberg, I. Z. & Walton, K. (1981). Relationship between presynaptic calcium current and postsynaptic potential in squid giant synapse. *Biophysical Journal* **33**, 323–352.

Llinas, R., Sugimori, M. & Silver, R. B. (1995). Time resolved calcium microdomains and synaptic transmission. *Journal de Physiologie* **89**, 77–81.

Miledi, R. (1973). Transmitter release induced by injection of calcium ions into nerve terminals. *Proceedings of the Royal Society* B **183**, 421–425.

Mulkey, R. M. & Zucker, R. S. (1993). Calcium released by photolysis of DM-nitrophen triggers transmitter release at the crayfish neuromuscular junction. *Journal of Physiology* **462**, 243–260.

Neher, E. & Augustine, G. J. (1992). Calcium gradients and buffers in bovine chromaffin cells. *Journal of Physiology* **450**, 273–301.

Parnas, H., Parnas I. & Segel, L. A. (1990). On the contribution of mathematical models to the understanding of neurotransmitter release. *International Review of Neurobiology* **32**, 1–46.

Parnas, H. & Segel, L. (1980). A theoretical explanation for some effects of calcium on the facilitation of neurotransmitter release. *Journal of Theoretical Biology* **84**, 3–29.

Parnas, I., Dudel, J., Parnas, H. & Ravin, R. (1996). Glutamate depresses release by activating non-conventional glutamate receptors at crayfish nerve terminals. *European Journal of Neuroscience* **8**, 116–126.

Parnas, I., Parnas, H. & Dudel, J. (1982). Neurotransmitter release and its facilitation in crayfish muscle. V. Basis for synapse differentiation of the fast and slow type in one axon. *Pflügers Archiv* **395**, 261–270.

Rahaminoff, R., Meiri, H., Erulkar, S. D. & Barenholz, Y. (1978). Changes in transmitter release induced by ion-containing liposomes. *Proceedings of the National Academy of Sciences of the USA* **75**, 5214–5216.

Simon, S. M. & Llinas, R. R. (1985). Compartmentalization of the submembrane calcium activity during calcium influx and its significance in transmitter release. *Biophysical Journal* **48**, 485–498.

Smith, S. J., Augustine, G. J. & Charlton, M. P. (1985). Transmission at voltage-clamped giant synapse of the squid: Evidence for cooperativity of presynaptic calcium action. *Proceedings of the National Academy of Sciences of the USA* **82**, 622–625.

Tank, D. W., Regehr, W. G. & Delaney, K. R. (1995). A quantitative analysis of presynaptic calcium dynamics that contribute to short-term enhancement. *Journal of Neuroscience* **15**, 7940–7952.

Wallin, B. G. (1967). Intracellular ion concentrations in single crayfish axons. *Acta Physiologica Scandinavica* **70**, 419–430.

Wojtowicz, J. M. & Atwood, H. L. (1984). Presynaptic potential and transmitter release at the crayfish neuromuscular junction. *Journal of Neurophysiology* **52**, 99–113.

Yamada, W. M. & Zucker, R. S. (1992). Time course of transmitter release calculated from simulations of a calcium diffusion model. *Biophysical Journal* **61**, 671–682.

Ziv, N. & Spira, M. E. (1993). Spatiotemporal distribution of $Ca^{2+}$ following axotomy and throughout the recovery process of cultured *Aplysia* neurons. *European Journal of Neuroscience* **5**, 657–668.

Ziv, N. & Spira, M. E. (1995). Axotomy induces a transient and localized elevation of free intracellular calcium concentration to the millimolar range. *Journal of Neurophysiology* **74**, 2625–2637.

Zucker, R. S., Delaney, K. R., Mulkey, R. & Tank, D. W. (1991). Presynaptic calcium in transmitter release and posttenanic potentiation. *Annals of the New York Academy of Sciences* **635**, 191–207.

**Acknowledgements**

This research was supported by the United States–Israel Binational Science Foundation (BSF) grant (no. 93-00308/1) to H. Parnas, I. Parnas and G. Augustine. We are grateful to the Goldie-Anna fund for continuous support. M. E. Spira is the Jacomo De Viali Professor for Neurobiology. I. Parnas is the Greenfield Professor for Neurobiology. We are grateful to Vladimir Litvak for his assistance in the graphic work.

**Author's email address**

I. Parnas: rea@vms.huji.ac.il

*Received 28 June 1996; accepted 25 February 1997.*